Journal of Applied Mechanical Engineering
ISSN: 2168-9873

Wu et al., J Appl Mech Eng 2016, 5:3
DOI: 10.4172/2168-9873.1000205

Research Article Open Access

Stress Fields Induced by Dislocation Loops in Isotropic CuNb Film-Substrate System

Wu W[1]*, Qian G[2] and Cui X[3]

[1]State Key Laboratory of Automotive Safety and Energy, Tsinghua University, Beijing 100084, PR China
[2]Paul Scherrer Institute, Nuclear Energy and Safety Department, Laboratory for Nuclear Materials, 5232 Villigen PSI, Switzerland
[3]Sustainable Energy Systems Group, Lawrence Berkeley National Laboratory, 1 Cyclotron Road MS 90R2002, Berkeley CA 94720, USA

Abstract

Based on linear superposition rules and fast discrete Fourier transformation, a semi-analytical solution is developed for calculating the elastic fields induced by dislocation loops in an isotropic thin film-substrate system. The elastic field problem of thin film-substrate system is decomposed into two sub-problems: bulk stress due to a dislocation loop in an infinite space, and correction stress induced by free surface and interface of the film-substrate system. Correction elastic field is linearly superimposed onto bulk elastic field to produce continuous displacement and traction stress across the interface plane of the perfectly-bounded film-substrate system. Firstly, calculation examples of dislocation loops in Cu-Nb film-substrate system are performed to demonstrate the calculation efficiency of the developed semi-analytical approach. Then, elastic fields of dislocation loops within Cu film and Nb substrate of the Cu-Nb film-substrate system are analyzed. Finally, effects of film thickness, loop positions are investigated, and it is found that the elastic fields of dislocation loop are influenced remarkably by these two factors.

Keywords: Elasticity; CuNb; Dislocation loop; Film-substrate; Isotropy

Introduction

Film-substrate structures and systems composed of thin film of finite thickness and substrate of infinite thickness are widely used in micro-chips, smart electronics, micro-sensors and manipulators, protective coatings, etc. During the industrial fabrication process and service life-time of film-substrate structures and systems, dislocation clusters will be generated and will result in the microstructure evolution of the film-substrate system. The performance, reliability and integrity of thin film-substrates are closely related to the material properties of the film and substrate, in particular, the crystal orientation (or texture for polycrystalline material), the dislocation density and distribution. Study of the collective dynamic behaviors of dislocations embedded in thin film-substrate system are of great interest to researchers and engineers, which are of critical importance for understanding the microstructure evolution, plastic deformation process of thin film-substrate systems.

Solutions to the elasticity field induced by dislocations within film-substrate system are important, because the elasticity solution provides a direct means of determining the Peach-Koehler force acting on dislocations, which is of direct relevance in understanding the microstructure evolution and mechanical behaviors of these film-substrate systems. In order to simulate the dynamic evolution process of dislocation and dislocation loops, accurate method are needed to calculate the stresses due to dislocations and dislocation loops in a heterogeneous thin film-substrate system. Making use of mirror dislocation concept and potential theory, Head [1,2] analyzed the changes in the stress field of a straight screw/edge dislocation caused by differences in the shear modulus on either side of bimetallic medium. Moreover, making use of image dislocation concepts, the equilibrium positions of a group of dislocations within bimaterial and film-substrate system are studied. It was found that when dislocations are located on the side with lower modulus and are situated on the slip plane which is perpendicular to the boundary of bimaterial system, dislocations are forced towards the boundary by an applied stress but repelled from the boundary by the change in modulus [3]. Making use of the solution of an edge dislocation in half-plane and that of the reversed traction force prescribed on the interface plane, Weeks et al. [4] presented an exact analysis for the elastic field and the Peach-Kohler force due to an edge dislocation within the substrate medium of film-substrate system. By using Fourier exponential transform, Lee and Dundurs [5] investigated the elastic field of an edge dislocation situated in the surface layer of the film-substrate system, and the behavior of edge dislocation is discussed through analyzing the Peach-Kochler force acting on these dislocations. By extending the classical mirror dislocation solutions for the interface plane between two semi-infinite elastically isotropic media, the image problem for a screw dislocation in the thin films of multilayered film-substrate system has been solved analytically [6], and the equilibrium position of a single dislocation in thin films was determined as a function of stress in the films. Kelly et al. [7] studied the stress field induced by an edge dislocation of arbitrary orientation in both the surface layer and substrate medium of the layer-substrate system, and the solution can be employed for deriving the solution of crack problems, together with the Peach-Koehler force. Savage [8] studied the solution for the displacement field induced by an edge dislocation in a layered half-space, and four elementary solutions were considered: the dislocation is either in the half-space or the layer, and the Burgers vector is either parallel or perpendicular to the interface plane. It was found that the surface displacement field produced by the edge dislocation in the layered half-space is very similar to that produced by an edge dislocation at a different depth in a uniform half-space. Moreover, a low-modulus (high-modulus) layer causes the equivalent dislocation in the half-space to appear shallower (deeper) than the actual dislocation in the layered half-space. Wu and Weatherly

***Corresponding author:** Wu W, State Key Laboratory of Automotive Safety and Energy, Tsinghua University, Beijing 100084, PR China, Tel: +8617710515502; E-mail: wenwang_wu@mail.tsinghua.edu.cn

Received February 15, 2016; **Accepted** March 16, 2016; **Published** March 19, 2016

Citation: Wu W, Qian G, Cui X (2016) Stress Fields Induced by Dislocation Loops in Isotropic CuNb Film-Substrate System. J Appl Mech Eng 5: 205. doi:10.4172/2168-9873.1000205

[9] studied the equilibrium position of misfit dislocations in epitaxial grown systems where the thickness of the epitaxial film is several orders of magnitude smaller than the thickness of the substrate. When the film is elastically stiffer than the substrate, the core of the dislocation is predicted to lie at some distance from the interface in the softer substrate. On the other hand, when the film is softer than the substrate, the core of the dislocation is always predicted to lie close to the interface [9]. The continuous dislocation image dislocation method is used to derive elastic solutions for an edge dislocation in an anisotropic film-substrate system, and it was found that elastic anisotropy and material mismatch play an important role in determining the image forces and the stress components due to an edge dislocation located in film-substrate systems [10]. The stress and displacement fields due to an edge dislocation in a linearly elastic isotropic film-substrate were studied based on image dislocations methods, and it was shown that the film thickness and dislocation position have a significant influence on the image force acting on the dislocation, and the film thickness variation due to an accumulation of dislocations may degrade the performance of optical films [11]. Recently, anisotropic elastic stress fields caused by a dislocation in Ge_xSi_{1-x} epitaxial layer on Si substrate are investigated by Wang [12], and effects of layer thickness, the dislocation position and the crystallographic orientation on the stresses of anisotropic film-substrate system were investigated extensively. It was revealed that the layer thickness and dislocation position strongly affects the stresses, while the crystallographic orientation play a very weak role in determining the elastic stress fields [12]. However, theses analytical solutions are mainly limited to straight dislocation lines parallel to the interface planes, which is invalid for curved dislocations and dislocation loops within film-substrate systems. Making use of potential theory and complete elliptic integrals, the elastic fields of a circular planar dislocation loop in an isotropic two-phase material, and the interaction forces between dislocation loop and the second phase were studied analytically, it was found that Peach-Koehler forces acting locally on the loop always tend to distort it [13,14]. Besides these analytical solutions, Weinberger et al. [15] and Wu et al. [16] developed semi-analytical solutions to calculate the image stress of approaching dislocations and dislocation loops within half space and free standing thin film. It is found that image force has a much stronger effect on 1/2 (111) dislocation loop in anisotropic (111) thin Fe foil, compared to the Voigt equivalent isotropy simulation results. Moreover, for complex dislocation configurations and boundary conditions, the image stress due to free surfaces and interfaces can now, owing to computing power, be computed by finite element method [16].

The objective of this paper is to develop an efficient and accurate method to calculate the stress due to dislocation loops in an isotropic heterogeneous thin film-substrate system, which is composed of a thin film of finite thickness and a substrate of infinite thickness. Based on linear superposition rules and fast discrete Fourier transformation, the problem is decomposed into two sub-problems: the stresses due to a dislocation loop in an infinite space and the correction stresses induced by the upper free surface of film and the film-substrate interface. Firstly, calculation examples of dislocation loops in Cu-Nb film-substrate system are performed to verify the semi-analytical approach; Then, elastic fields of dislocation loops within Cu film and Nb substrate of the Cu-Nb film-substrate system are analyzed; Finally, effects of film thickness, dislocation loop positions on the elastic field of is investigated, and it is found that film thickness, dislocation loop positions has a remarkable impact on the elastic fields of dislocation loops within film-substrate system.

Stress Fields Induced by Dislocation Loop in Perfect Bonding Film-Substrate System

Statement of problem

As shown in Figure 1, perfect bonding isotropic film-substrate system is decomposed into a thin film (**A**) of finite thickness 2h and a substrate (B) of infinite thickness. The elastic properties of the film and substrate medium are assumed to be (λ_f, μ_f, v_f) and (λ_s, μ_s, v_s), respectively. Two sets of local Cartesian coordinates are employed for describing the film-substrate system: local Cartesian coordinate (x^+,y^+,z^+) for the upper thin film A, and local Cartesian coordinate (x^-,y^-,z^-) for the lower substrate half space B, where (x^+, y^+) and (x^-,y^-) are parallel to the interface plane and simplified as (x,y). The origin of the local Cartesian coordinate for the upper thin film A is located in the middle of the thin film, and the origin of the local Cartesian coordinate for the lower substrate B is located on the interface plane. Accordingly, $-h \le z^+ \le h$ is valid for the upper thin film A, and $z^- \le 0$ is valid for the lower substrate B. Dislocation loop L_1 is located in the thin film medium A, and dislocation loop L_2 is located in the substrate medium B.

The free surface and interface of the perfect bonding film-substrate system should satisfy the following requirements:

(a) Free traction stress should be satisfied on the top free surface of the film-substrate system.

$$\sigma_{i3}^{f}\Big|_{z^+=+h} = 0 \tag{1}$$

(b) Elastic displacement and traction stress should be continuous across the interface planes of the film-substrate system.

$$\sigma_{i3}^{f}\Big|_{z^+=-h} = \sigma_{i3}^{s}\Big|_{z^-=0} \tag{2}$$

and

$$u_{i}^{f}\Big|_{z^+=-h} = u_{i}^{s}\Big|_{z^-=0} \tag{3}$$

Where 'f' and 's' stand for the film and substrate, and superscripts '+' and '–' distinguish the local Cartesian coordinates of the film and substrate, respectively.

Solution for Perfect Bonding Film-Substrate System

In this subsection, a semi-analytical solution is proposed to solve the elastic fields due to dislocation loops within thin film or substrate of perfect bonding film-substrate system. Elastic field of perfect bonding film-substrate system can be decomposed into two sub-problems: bulk stress due to a dislocation loop in an infinite space, and correction stress induced by the free surface and interface of the film-substrate system.

As shown in Figure 2a, perfect bonding film-substrate system is

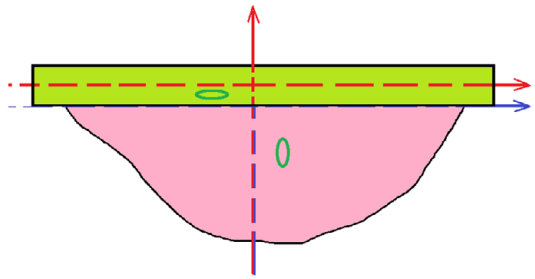

Figure 1: Cartesian coordinates of a film-substrate system: (a) coordinate (x^+,y^+,z^+) for the thin film; (b) coordinate (x^-,y^-,z^-) for the lower half space.

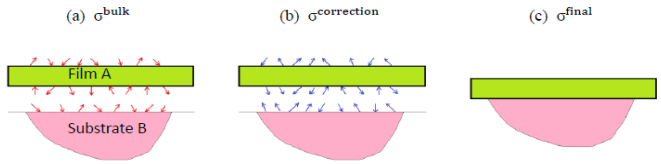

Figure 2: Diagram of decomposition of film-substrate system containing dislocation loops L_1 within the upper thin foil A and dislocation loops L_2 with the lower layer B into a two-step linear superposition problem: (a), bulk stress and $\{\sigma_{ij}\}_A^{bulk}$; (b), correction traction stress $\{\sigma_{i3}\}_A^{correction}$ and $\{\sigma_{i3}\}_B^{correction}$; (c), continuous interface displacement and traction stress are generated at interface plane; and free traction boundary conditions are satisfied on the top surface planes of the film-substrate system.

decomposed into thin film **A** containing dislocation loops L_1 and substrate B containing dislocation loop L_2. Bulk traction elastic field $\{\sigma_{i3}\}_A^{\infty}$ and $\{\sigma_{i3}\}_B^{\infty}$ on the top free surface and interface plane can be calculated out.

As shown in Figure 2b, correction traction stress $\{\sigma_{i3}\}_A^{correction}$ and $\{\sigma_{i3}\}_B^{correction}$ are linearly superimposed onto the bulk elastic fields.

As shown in Figure 2c, after linear superposition of bulk stress and correction stress, displacement and traction stress continuity across the interface plane are satisfied.

Elastic Fields of Dislocation Loops within Infinite Isotropic Medium

Bulk displacement of dislocation loops can be calculated with Volterra's formula, and written as surface integration over dislocation area [17,18]:

$$u_m^{\infty}(x) = b_i \int_S C_{ijkl} G_{km,l}(x - x') dS_j \tag{4}$$

Where S is the dislocation surface, a cap with its boundary formed by dislocation loop perimeter. C_{ijkl} are the elastic constants, and $G_{km,l}$ is the first order derivative of Green's function.

For an isotropic material, following relation exists:

$$b_i C_{ijkl} G_{km,l}(R) = \frac{1}{8\pi\mu}\left[\begin{array}{l}\mu b_m R_{,ppj} + \mu\left(b_l R_{,ppl}\delta_{jm} - b_j R_{,ppm}\right) \\ +2\left(\frac{\lambda+\mu}{\lambda+2\mu}\right)\mu\left(b_j R_{,ppm} - b_i R_{,mij}\right)\end{array}\right] \tag{5}$$

Where R = x–x′ is the vector from dislocation position x′ to the calculated position x, λ, is Lamé's first parameter of isotropic material, and μ is shear modulus of isotropic material, δ_{ij} is the Kronecker delta operator.

Bulk stress induced by dislocation loops in a homogenous medium can be calculated with Mura's formula [18]. Firstly, bulk displacement gradient can be written as:

$$u_{i,j}^{\infty}(x) = \int \varepsilon_{jnh} C_{pqmn} G_{ip,q}(x - x') b_m' dx_h' \tag{6}$$

where the integration is performed along dislocation loop perimeter.

For an isotropic material, it appears that:

$$C_{pqmn} G_{ip,q}(x - x') = \frac{-1}{8\pi(1-\nu)}\left[\begin{array}{l}(1-2\nu)\frac{\delta_{ni}(x_m - x_m') + \delta_{im}(x_n - x_n') + \delta_{mn}(x_i - x_i')}{R^3} \\ +3\frac{(x_m - x_m')(x_n - x_n')(x_i - x_i')}{R^5}\end{array}\right] \tag{7}$$

Where R = |X-X′| is the distance from the dislocation position x′ to the calculated position x in the space.

Considering the displacement-strain differential relation, bulk stress of dislocation segment can be generated with isotropic Hooke's law:

$$\sigma_{ij}^{\infty} = \lambda.\varepsilon_{kk}.\delta_{ij} + 2\mu\varepsilon_{ij} = C_{ijkl}.\varepsilon_{ij} \tag{8}$$

Then, bulk stress induced by a circular dislocation loop can be produced through linear integration along dislocation loop perimeter for a round.

Correction Stress of Lower Substrate Medium

In the absence of body forces, the stress equilibrium equation of the lower substrate medium B can be written in terms of the displacement $u_i^-(x)$ as:

$$\mu^s u_{i,jj}^- + \left(\lambda^s + \mu^s\right) u_{j,ji}^- = 0 \tag{9}$$

Where $\lambda^s = 2\mu^s\nu^s/(1-2\nu^s)$, μ^s and ν^s are the shear modulus and Poisson's ratio for the lower substrate medium B.

Similar to the solutions for the image stress of half space developed by Weinberger et. al [15], an arbitrary correction elastic field written in the form of Fourier series with unknown Fourier coefficients is employed for solving the correction elastic field of the lower substrate medium B. The following correction displacement solution to Eq. (9) is written as sum over different Fourier modes:

$$\left\{\begin{array}{l}u^- = \sum_{k_x}\sum_{k_y}\left(+k_x z^- K_1^- - k_y K_2^- + ik_x K_3^-\right)\cdot e^{+k_z z^-}\cdot e^{+\left(ik_x x + ik_y y\right)} \\ v^- = \sum_{k_x}\sum_{k_y}\left(+k_y z^- K_1^- + k_x K_2^- + ik_y K_3^-\right)\cdot e^{+k_z z^-}\cdot e^{+\left(ik_x x + ik_y y\right)} \\ w^- = \sum_{k_x}\sum_{k_y}\left(\left(-ik_x z^- + i\frac{\ddot{e}_s + 3\dot{i}_s}{\ddot{e}_s + \dot{i}_s}\right)K_1^- + k_z K_3^-\right)\cdot e^{+k_z z^-}\cdot e^{+\left(ik_x x + ik_y y\right)}\end{array}\right. \tag{10}$$

where $k_z = \sqrt{k_x^2 + k_y^2}$ and $\left(K_1^-, K_2^-, K_3^-\right)$ are complex constants. The solution is periodic in the x and y directions and exponential in the z^- direction.

Due to the completeness of the Fourier series, Fourier coefficient components for certain (k_x, k_y) mode can be written as:

$$\left\{\begin{array}{l}\hat{u}^- = \left(+k_x z^- K_1^- - k_y K_2^- + ik_x K_3^-\right)\cdot e^{+k_z z^-} \\ \hat{v}^- = \left(+k_y z^- K_1^- + k_x K_2^- + ik_y K_3^-\right)\cdot e^{+k_z z^-} \\ \hat{w}^- = \left(\left(-ik_x z^- + i\frac{\ddot{e}_s + 3\dot{i}_s}{\ddot{e}_s + \dot{i}_s}\right)K_1^- + k_z K_3^-\right)\cdot e^{+k_z z^-}\end{array}\right. \tag{11}$$

Thus, the correction displacement field is written as:

$$u_i^-\left(x, y, z^-\right) = \sum_{k_x^-}\sum_{k_y^-}\hat{u}_i^-\left(k_x, k_y, z^-\right).e^{+\left(ik_x x + ik_y y\right)} \tag{12}$$

The correction displacement components $\left(\hat{u}^-, \hat{v}^-, \hat{w}^-\right)$ on the free surface plane $z^- = 0$ for certain (k_x, k_y) mode can be written as:

$$\begin{Bmatrix}\hat{u}^-\\ \hat{v}^-\\ \hat{w}^-\end{Bmatrix}=\left[N^-\right]\cdot\begin{Bmatrix}K_1^-\\ K_2^-\\ K_3^-\end{Bmatrix} \tag{13}$$

where the details of $[N^-]$ are shown in Appendix (A. 1).

Following the displacement field solution in Eq. (10), it is straightforward to obtain the strain field $\hat{\varepsilon}_{ij}^-$ through differentiation rule and the stress field $\hat{\sigma}_{ij}^-$ by using Hooke's law. The traction stress field can also be written in the form of Fourier series:

$$\sigma_{i3}^-\left(x,y,z^-\right)=\sum_{k_x}\sum_{k_y}\hat{\sigma}_{i3}^-\left(k_x,\ k_y,z^-\right)\cdot e^{+\left(ik_x x+ik_y y\right)} \tag{14}$$

The correction traction stress components $\left(\hat{\sigma}_{13}^-,\hat{\sigma}_{23}^-,\hat{\sigma}_{33}^-\right)$ on the free surface plane $z^-=0$ for certain $\left(k_x,k_y\right)$ mode can be written as:

$$\begin{Bmatrix}\hat{\sigma}_{13}^-\\ \hat{\sigma}_{23}^-\\ \hat{\sigma}_{33}^-\end{Bmatrix}=\left[M^-\right]\cdot\begin{Bmatrix}K_1^-\\ K_2^-\\ K_3^-\end{Bmatrix} \tag{15}$$

and the details of $\left[M^-\right]$ are shown in Appendix (A. 2).

The numerical solutions of Eqs. (10)-(15) for the substrate medium are considered in the x and y directions with periodic lengths L_x and L_y. The wave number is set to be $k_x=2\pi n_x/L_x$ and $k_y=2\pi n_y/L_y$, where $n_x=n_y=0,\pm1,\ 2,\pm3\ldots$

Correction Stress of upper Thin Film

Similar to the efficient semi-analytical image stress solution derived by Weinberger et al. [15] of isotropic thin foils, an arbitrary correction elastic field written in the form of Fourier series with unknown Fourier coefficients is employed for solving the correction elastic field of the film medium A.

In the absence of body forces, the stress equilibrium of an isotropic linear medium composed of upper thin film medium **A** can be written in terms of the displacement $u_i^+(x)$ as:

$$\mu^f u_{i,jj}^+ +\left(\lambda^f+\mu^f\right)u_{j,ji}^+=0 \tag{16}$$

where $\lambda^f=2\mu^f\nu^f/\left(1-2\nu^f\right)$, μ^f and ν^f are the shear modulus and Poisson's ratio for the upper thin film medium A. The thin film is assumed to have a thickness of 2h in the z^+ direction, and $-h\ z^+\le h$.

The correction elastic field can be written as sum over Fourier series, and the solution is periodic in the x and y directions, and hyperbolic in the z^+ direction.

$$\begin{cases}u^+=\sum_{k_x}\sum_{k_y}\begin{bmatrix}\left(k_xz^+A-k_yF+ik_xG\right)sinh\left(k_zz^+\right)\\ +\left(k_xz^+E+k_yB+ik_xC\right)cosh\left(k_zz^+\right)\end{bmatrix}\cdot e^{\left(ik_xx+ik_yy\right)}\\ v^+=\sum_{k_x}\sum_{k_y}\begin{bmatrix}\left(k_yz^+A+k_xF+ik_yG\right)sinh\left(k_zz^+\right)\\ +\left(k_yz^+E-k_xB+ik_yC\right)cosh\left(k_zz^+\right)\end{bmatrix}\cdot e^{\left(ik_xx+ik_yy\right)}\\ w^+=\sum_{k_x}\sum_{k_y}\begin{bmatrix}\left(-ik_zz^+A+i\frac{\ddot{e}_f+3\dot{i}_f}{\ddot{e}_f+\dot{i}_f}E+k_zG\right)cosh\left(k_zz^+\right)\\ +\left(-ik_zz^+E+i\frac{\ddot{e}_f+3\dot{i}_f}{\ddot{e}_f+\dot{i}_f}A+k_zC\right)sinh\left(k_zz^+\right)\end{bmatrix}\cdot e^{\left(ik_xx+ik_yy\right)}\end{cases} \tag{17}$$

where $k_z=\sqrt{k_x^2+k_y^2}$, and the unknown terms (A,B,C) and (E,F,G) are complex constants.

Due to the mathematical completeness of Fourier series, the Fourier coefficient components for each Fourier (k_x, k_y) mode is:

$$\begin{cases}\hat{u}^+=\begin{bmatrix}\left(k_xz^+A-k_yF+ik_xG\right)sinh\left(k_zz^+\right)\\ +\left(k_xz^+E+k_yB+ik_xC\right)cosh\left(k_zz^+\right)\end{bmatrix}\\ \hat{v}^+=\begin{bmatrix}\left(k_yz^+A+k_xF+ik_yG\right)sinh\left(k_zz^+\right)\\ +\left(k_yz^+E-k_xB+ik_yC\right)cosh\left(k_zz^+\right)\end{bmatrix}\\ \hat{w}^+=\begin{bmatrix}\left(-ik_zz^+A+i\frac{\ddot{e}_f+3\dot{i}_f}{\ddot{e}_f+\dot{i}_f}E+k_zG\right)cosh\left(k_zz^+\right)\\ +\left(-ik_zz^+E+i\frac{\ddot{e}_f+3\dot{i}_f}{\ddot{e}_f+\dot{i}_f}A+k_zC\right)sinh\left(k_zz^+\right)\end{bmatrix}\end{cases} \tag{18}$$

Alternatively, the correction displacement field in Eq. (17) can be written as:

$$u_i^+\left(x,y,z^+\right)=\sum_{k_x}\sum_{k_y}\left[\hat{u}_i^+\left(k_x,k_y,z^+\right)\right].\exp\left(ik_xx+ik_yy\right) \tag{19}$$

and the correction traction stress can be obtained from isotropic Hooke's law:

$$\sigma_{i3}^+\left(x,y,z^+\right)=\sum_{k_x}\sum_{k_y}\left[\hat{\sigma}_{i3}^+\left(k_x,k_y,z^+\right)\right].\exp\left(ik_xx+ik_yy\right) \tag{20}$$

Then, Eq. (20) was submitted into the equilibrium Eq. (16), correction displacement fields on the surface planes $z^+=\pm h$ can be combined together, and rewritten into two sets of equations on unknown coefficients (A,B,C) and (E,F,G), which correspond to the symmetrical and the asymmetrical parts, respectively.

The symmetrical correction displacement is:

$$u^S=\frac{1}{2}\begin{bmatrix}\hat{u}^+\big|_{z^+=+h}+\hat{u}^+\big|_{z^+=-h}\\ \hat{v}^+\big|_{z^+=+h}+\hat{v}^+\big|_{z^+=-h}\\ \hat{w}^+\big|_{z^+=+h}-\hat{w}^+\big|_{z^+=-h}\end{bmatrix}=\left[N^S\right]\cdot\begin{Bmatrix}A\\ B\\ C\end{Bmatrix}\cdot\exp\left(ik_xx+ik_yy\right) \tag{21}$$

and the asymmetrical correction displacement part is:

$$u^A=\frac{1}{2}\begin{bmatrix}\hat{u}^+\big|_{z^+=+h}-\hat{u}^+\big|_{z^+=-h}\\ \hat{v}^+\big|_{z^+=+h}-\hat{v}^+\big|_{z^+=-h}\\ \hat{w}^+\big|_{z^+=+h}+\hat{w}^+\big|_{z^+=-h}\end{bmatrix}=\left[N^A\right]\cdot\begin{Bmatrix}E\\ F\\ G\end{Bmatrix}\cdot\exp\left(ik_xx+ik_yy\right) \tag{22}$$

The symmetrical correction traction stress is:

$$T^S=\frac{1}{2}\begin{bmatrix}\sigma_{13}^+\big|_{z^+=+h}-\sigma_{13}^-\big|_{z^+=-h}\\ \sigma_{23}^+\big|_{z^+=+h}-\sigma_{23}^-\big|_{z^+=-h}\\ \sigma_{33}^+\big|_{z^+=+h}+\sigma_{33}^-\big|_{z^+=-h}\end{bmatrix}=\left[M^S\right]\cdot\begin{Bmatrix}A\\ B\\ C\end{Bmatrix}\cdot\exp\left(ik_xx+ik_yy\right) \tag{23}$$

and the asymmetrical correction traction stress is:

$$T^A=\frac{1}{2}\begin{bmatrix}\sigma_{13}^+\big|_{z^+=+h}+\sigma_{13}^-\big|_{z^+=-h}\\ \sigma_{23}^+\big|_{z^+=+h}+\sigma_{23}^-\big|_{z^+=-h}\\ \sigma_{33}^+\big|_{z^+=+h}-\sigma_{33}^-\big|_{z^+=-h}\end{bmatrix}=\left[M^A\right]\cdot\begin{Bmatrix}E\\ F\\ G\end{Bmatrix}\cdot\exp\left(ik_xx+ik_yy\right) \tag{24}$$

The explicit expressions for the correction displacement and traction stress matrices $[M^S]$, $[M^A]$, $[N^S]$ and $[N^A]$ are given in Appendix (A. 3) - (A. 6).

The calculation procedures of Eqs. (17)-(24) for isotropic thin film

are considered in the x and y directions with periodic lengths L_x and L_y. The wave number is set to be $k_x = 2\pi n_x/L_x$ and $k_y = 2\pi n_y/L_y$, where $n_x = n_y = 0, \pm1, \pm2, \pm3\ldots$

Elastic Field of Perfect Bonding Film-Substrate System

Considering the displacement and traction stress continuity requirements in Eqs. (1)-(3) for the perfect bonding film-substrate system, following relation stands for each (k_x, k_y) Fourier mode.

Free traction stress on the free surface plane of the perfect bonding film-substrate system should be satisfied:

$$\left\{\hat{\sigma}_{i3}\right\}^{\infty}_{z^+=+h} + \left\{\hat{\sigma}_{i3}\right\}^{\text{correction}}_{z^+=+h} = 0 \tag{25}$$

Interface traction stress and displacement continuity across the interface plane of the perfect bonding film-substrate system should be satisfied:

$$\left\{\hat{\sigma}_{i3}\right\}^{\infty}_{z^+=-h} + \left\{\hat{\sigma}_{i3}\right\}^{\text{correction}}_{z^+=-h} = \left\{\hat{\sigma}_{i3}\right\}^{\infty}_{z^-=0} + \left\{\hat{\sigma}_{i3}\right\}^{\text{correction}}_{z^-=0} \tag{26}$$

and

$$\left\{\hat{u}_{i}\right\}^{\infty}_{z^+=+h} + \left\{\hat{u}_{i}\right\}^{\text{correction}}_{z^+=+h} = \left\{\hat{u}_{i}\right\}^{\infty}_{z^-=0} + \left\{\hat{u}_{i}\right\}^{\text{correction}}_{z^-=0} \tag{27}$$

After submitting the bulk elastic field and correction elastic field into Eqs. (25)-(27), the following relations stand for each (k_x, k_y) Fourier mode.

(a) Free traction boundary condition should be satisfied on the top free surface plane of the thin film A for each (k_x, k_y) Fourier mode.

$$\left[M^S\right]\begin{Bmatrix}A\\B\\C\end{Bmatrix} + \left[M^A\right]\begin{Bmatrix}E\\F\\G\end{Bmatrix} + \begin{bmatrix}\{\hat{\sigma}_{13}\}^{\infty}_{z^+=h}\\ \{\hat{\sigma}_{23}\}^{\infty}_{z^+=h}\\ \{\hat{\sigma}_{33}\}^{\infty}_{z^+=h}\end{bmatrix} = 0 \tag{28}$$

(b) Interface traction stress should be continuous for each (k_x, k_y) Fourier mode.

$$\left[K_{ij}\right]*\left[-\left[M^S\right]\begin{Bmatrix}A\\B\\C\end{Bmatrix} + \left[M^A\right]\begin{Bmatrix}E\\F\\G\end{Bmatrix}\right] + \begin{bmatrix}\{\hat{\sigma}_{13}\}^{\infty}_{z^+=-h}\\ \{\hat{\sigma}_{23}\}^{\infty}_{z^+=-h}\\ \{\hat{\sigma}_{33}\}^{\infty}_{z^+=-h}\end{bmatrix} = \left[M^-\right]\begin{Bmatrix}K_1^-\\K_2^-\\K_3^-\end{Bmatrix} + \begin{bmatrix}\{\hat{\sigma}_{13}\}^{\infty}_{z^-=0}\\ \{\hat{\sigma}_{23}\}^{\infty}_{z^-=0}\\ \{\hat{\sigma}_{33}\}^{\infty}_{z^-=0}\end{bmatrix} \tag{29}$$

in which, $\left[K_{ij}\right] = \text{diag}\{1, 1, -1\}$ is a 3*3 diagonal matrix.

(c) Interface displacement should be continuous for each (k_x, k_y) Fourier mode.

$$\left[K_{ij}\right]*\left[\left[N^S\right]\begin{Bmatrix}A\\B\\C\end{Bmatrix} - \left[N^A\right]\begin{Bmatrix}E\\F\\G\end{Bmatrix}\right] + \begin{bmatrix}\{\hat{u}_1\}^{\infty}_{z^+=-h}\\ \{\hat{u}_2\}^{\infty}_{z^+=-h}\\ \{\hat{u}_3\}^{\infty}_{z^+=-h}\end{bmatrix} = \left[N^-\right]\begin{Bmatrix}K_1^-\\K_2^-\\K_3^-\end{Bmatrix} + \begin{bmatrix}\{\hat{u}_1\}^{\infty}_{z^-=0}\\ \{\hat{u}_2\}^{\infty}_{z^-=0}\\ \{\hat{u}_3\}^{\infty}_{z^-=0}\end{bmatrix} \tag{30}$$

In summary, Eqs. (28)-(30) can be written together as:

$$\begin{bmatrix}\left[M^S\right] & \left[M^A\right] & 0\\ \left[K_{ij}\right]*\left[N^S\right] & -\left[K_{ij}\right]*\left[N^A\right] & -\left[N^-\right]\\ -\left[K_{ij}\right]*\left[M^S\right] & \left[K_{ij}\right]*\left[M^A\right] & -\left[M^-\right]\end{bmatrix}\begin{Bmatrix}A\\B\\C\\E\\F\\G\\K_1^-\\K_2^-\\K_3^-\end{Bmatrix} = \begin{Bmatrix}-\{\hat{\sigma}_{13}\}^{\infty}_{z^+=h}\\ -\{\hat{\sigma}_{23}\}^{\infty}_{z^+=h}\\ -\{\hat{\sigma}_{33}\}^{\infty}_{z^+=h}\\ -\{\hat{u}_1\}^{\infty}_{z^+=-h} + \{\hat{u}_1\}^{\infty}_{z^-=0}\\ -\{\hat{u}_2\}^{\infty}_{z^+=-h} + \{\hat{u}_2\}^{\infty}_{z^-=0}\\ -\{\hat{u}_3\}^{\infty}_{z^+=-h} + \{\hat{u}_3\}^{\infty}_{z^-=0}\\ -\{\hat{\sigma}_{13}\}^{\infty}_{z^+=-h} + \{\hat{\sigma}_{13}\}^{\infty}_{z^-=0}\\ -\{\hat{\sigma}_{23}\}^{\infty}_{z^+=-h} + \{\hat{\sigma}_{23}\}^{\infty}_{z^-=0}\\ -\{\hat{\sigma}_{33}\}^{\infty}_{z^+=-h} + \{\hat{\sigma}_{33}\}^{\infty}_{z^-=0}\end{Bmatrix} \tag{31}$$

Then, unknown coefficient (A,B,C,E,F,G) and $\left(K_1^-, K_2^-, K_3^-\right)$ of correction displacement can be solved from Eq. (31), and the correction elastic field of the film medium A and substrate medium B can be generated.

The total elastic field is the sum of the two contribution parts: bulk elastic field $\left\{\hat{\sigma}_{ij}\right\}^{\text{bulk}}_{A}$ and $\left\{\hat{\sigma}_{ij}\right\}^{\text{bulk}}_{B}$; and correction elastic fields $\left\{\hat{\sigma}_{ij}\right\}^{\text{correction}}_{A}$ and $\left\{\hat{\sigma}_{ij}\right\}^{\text{correction}}_{B}$, respectively.

Total displacement within the upper film A of the film-substrate system is:

$$\left\{\hat{u}_{i}\right\}^{\text{final}}_{A} = \left\{\hat{u}_{i}\right\}^{\text{bulk}}_{A} + \left\{\hat{u}_{i}\right\}^{\text{correction}}_{A} \tag{32}$$

Total stress within the upper film A of the film-substrate system is:

$$\left\{\hat{\sigma}_{ij}\right\}^{\text{final}}_{A} = \left\{\hat{\sigma}_{ij}\right\}^{\text{bulk}}_{A} + \left\{\hat{\sigma}_{ij}\right\}^{\text{correction}}_{A} \tag{33}$$

Total displacement within the substrate B of the film-substrate system is:

$$\left\{\hat{u}_{i}\right\}^{\text{final}}_{B} = \left\{\hat{u}_{i}\right\}^{\text{bulk}}_{B} + \left\{\hat{u}_{i}\right\}^{\text{correction}}_{B} \tag{34}$$

Total stress within the substrate B of the film-substrate system is:

$$\left\{\hat{\sigma}_{ij}\right\}^{\text{final}}_{B} = \left\{\hat{\sigma}_{ij}\right\}^{\text{bulk}}_{B} + \left\{\hat{\sigma}_{ij}\right\}^{\text{correction}}_{B} \tag{35}$$

Calculation Examples

In this section, the above semi-analytical approach is employed for analyzing the elastic fields induced by dislocation loop within perfect bonding isotropic Cu-Nb film-substrate system. The local Cartesian coordinate (x^+, y^+, z^+) is along $(11\bar{2})$, $(\bar{1}10)$ and (111) in upper Cu thin foil; and the local Cartesian coordinate (x^-, y^-, z^-) is along $(1\bar{1}2)$, $(1\bar{1}\bar{1})$ and (110) in lower Nb substrate medium. The origin of the upper Cartesian coordinate is in the middle of the Cu thin foil, and the origin of the lower Nb half space is on the interface plane of the film-substrate system. In all the calculation examples below, dislocation loop is segmented into 40 straight dislocation segments along the circular perimeter for a round, and bulk displacement and stress fields are obtained through integrating the dislocation segments around the dislocation loop perimeter, based on Volterra's [17], Devincre's [18] and Mura's integration formulas [19], respectively. The elastic modulus of Cu and Nb is shown in Table 1, and the isotropic equivalent shear modulus and Poisson's ratio are treated with Voigt isotropic model [20,21]. In the following simulation examples, the periodic length on the interface plane is $L_x = L_y = 200$ nm, the meshing density is $n_x = n_y = 200$, and the Fourier wave number range is: $-30 \le k_x \le 30$ and $-30 \le k_y \le 30$.

Elastic Field due to a Dislocation Loop in the Substrate Medium

In this section, elastic displacement and traction stress due to a dislocation loop in the lower Nb substrate medium of the perfect bonding Cu-Nb film-substrate system are studied, and the thickness of the upper Cu film is assumed to be 40 nm. The circular 1/2a⟨110⟩(111)

Material	C_{11} (GPa)	C_{12} (GPa)	C_{14} (GPa)	Voigt shear modulus (GPa)	Voigt Poisson's ratio (-)	Lattice constant (nm)
Cu	168.4	121.4	75.4	54.64	0.3241	a=0.36149
Nb	240.2	125.6	28.2	39.84	0.3875	a=0.33004

Table 1: Elastic parameters of pure Cu and Nb [20,21].

dislocation loop with radius r = 5 nm is located at a distance d = 10 nm below the interface plane in lower Nb medium, and its habit plane is inclined to the interface plane. Figures 3a, 3b, 3e and 3f are the side view of the elastic field plotted in the σ_{xz} plane (y = 0), and Figures 3c and 3d are the side view of the elastic field plotted in the oyz plane (x = 0) for the perfect bonding Cu-Nb film-substrate system. It can be seen that the final interface in plane and out of plane displacement field, traction stress field across the interface plane are identical, and thus continuous displacement and traction stress is generated.

As shown in Figure 4, correction elastic field are superimposed onto the bulk elastic field, thus generating the final interface elastic field, and the contributions from bulk and correction elastic fields are compared with each other. As shown in Figures 4a-4f, interface displacement profile of u and w, and interface traction stress σ_{xz} and σ_{zz} are plotted along x direction (y = 0) on the interface plane of the perfect bonding Cu-Nb film-substrate system; as shown in Figures 4c and 4d, interface displacement profile of v and interface traction stress σ_{yz} are plotted along y direction (x = 0) on the interface plane of the perfect bonding Cu-Nb film-substrate system. It can be seen from Figures 4b, 4d and 4f that the amplitudes of bulk traction stress are slightly strengthened on the interface plane, as the Voigt shear modulus of upper layer Cu is larger than lower layer Nb, and the traction stress due to a dislocation loop in the lower substrate Nb is slightly strengthened by the upper Cu film at the perfect bonding interface plane.

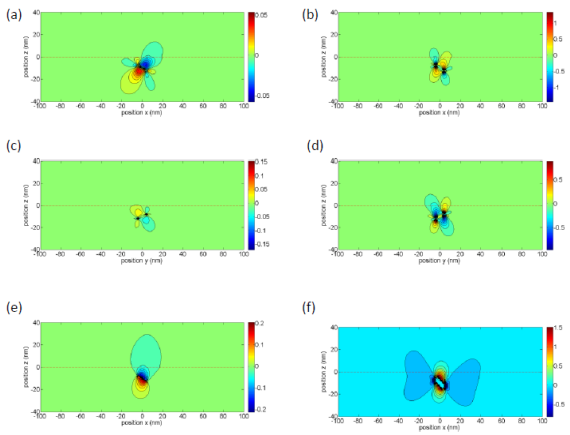

Figure 3: Elastic fields due to a dislocation loop in the lower Nb substrate of the perfect bonding Cu–Nb film-substrate system: displacement field (a) u ^{final}; (c), v ^{final}; (e) w ^{final} (in unit: nm); traction stress (b) σ_{xz}^{final} ; (d), σ_{yz}^{final} ; (f) σ_{zz}^{final} (in unit: GPa).

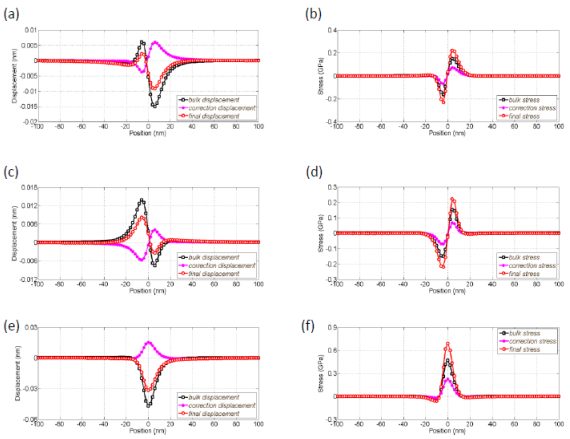

Figure 4: Elastic profile due to a dislocation loop in the lower Nb substrate of the perfect bonding Cu–Nb film-substrate system: displacement profile (a) u ^{final}; (c) v ^{final}; (e) w ^{final} (in unit: nm); traction stress profile (b) σ_{xz}^{final} ; (d) σ_{yz}^{final} ; (f) σ_{zz}^{final} (in unit: GPa).

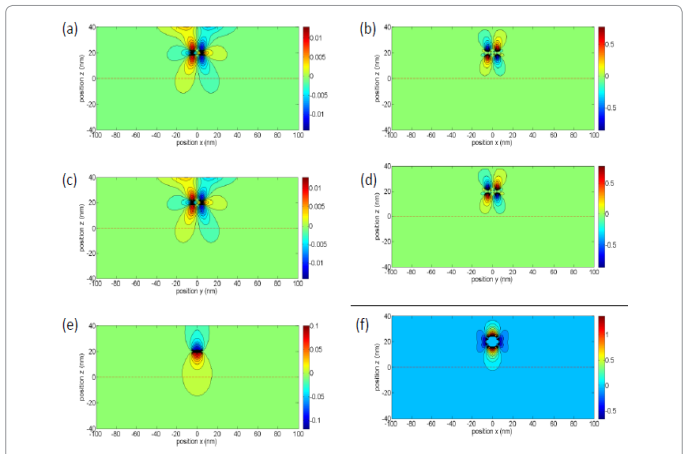

Figure 5: Elastic fields due to a dislocation loop in the upper Cu film of the perfect bonding Cu–Nb film-substrate system: displacement field (a) u ^{final}; (c) v ^{final}; (e) w ^{final} (in unit: nm); traction stress (b) σ_{xz}^{final} ; (d) σ_{yz}^{final} ; (f) σ_{zz}^{final} (in unit: GPa).

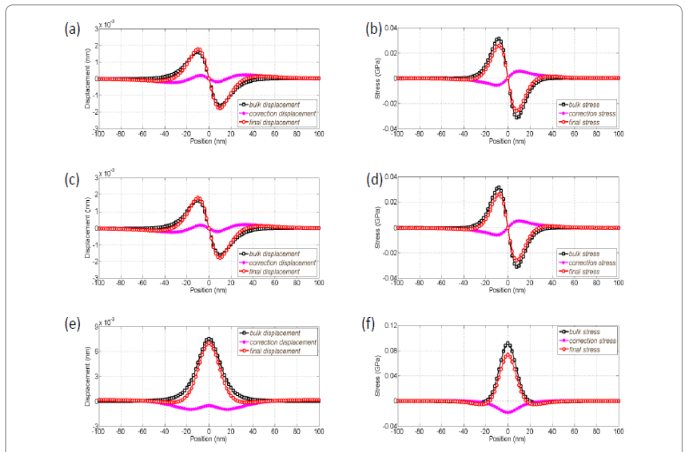

Figure 6: Elastic profile due to a dislocation loop in the upper Cu film of the perfect bonding Cu–Nb film-substrate system: displacement profile (a) u ^{final}; (c) v ^{final}; (e) w ^{final} (in unit: nm); traction stress profile (b) σ_{xz}^{final} ; (d) σ_{yz}^{final} ; (f) σ_{zz}^{final} (in unit: GPa).

Elastic Field due to a Dislocation Loop in the Film Medium

In this section, elastic displacement and traction stress due to a dislocation loop in the upper Cu film of the perfect bonding Cu-Nb film-substrate system are studied, and the thickness of the upper Cu film is assumed to be 40 nm. The circular 1/3a(111)(111) dislocation loop with radius r = 5 nm is located in the middle of upper Cu thin film, and its habit plane is parallel to the interface plane. Figures 5a, 5b, 5e and 5f are the side view of the elastic field plotted in the oxz plane (y = 0), and Figures 5c and 5d are the side view of the elastic field plotted in the oyz plane (x = 0) for the perfect bonding Cu-Nb film-substrate system. It can be seen that the final interface in plane and out of plane displacement field, traction stress field across the interface plane are

identical, and thus continuous displacement and traction stress is generated.

As shown in Figures 6a, 6b, 6e and 6f, interface displacement profile of u and w, and interface traction stress σ_{xz} and σ_{zz} are plotted along x direction (y = 0) on the interface plane of the perfect bonding Cu-Nb film-substrate system; as shown in Figures 6c and 6d, interface displacement profile of v and interface traction stress σ_{yz} are plotted along y direction (x = 0) on the interface plane of the perfect bonding Cu-Nb film-substrate system. It can be seen from Figures 6b, 6d and 6f that the amplitudes of bulk traction stress are slightly weakened on the interface plane, as the Voigt shear modulus of upper layer Cu is larger than lower layer Nb, and the traction stress due to a dislocation loop in the upper Cu film is slightly weakened by the lower Nb substrate at the perfect bonding interface plane.

Film Thickness Effect on Elastic Field of a Dislocation Loop in the Film Medium

In this subsection, effects of film thickness on the interface displacement and interface traction stress amplitudes are investigated. Besides Cu film thickness, the physical and material parameters of dislocation loop and film-substrate system are identical to the simulated Cu-Nb film-substrate system example in subsection 3.2. The thin Cu film thickness is assumed to be: t = 20, 30, 40, 50 and 60 nm, and the dislocation loop is situated in the middle of the upper thin Cu film. The simulation results are shown in Figure 7, and side view of the traction stress σ_{xz} and σ_{zz} are plotted in the oxz plane (y = 0) for the perfect bonding Cu-Nb film-substrate system. It can be concluded from Figure 7 that: with the decrease of film thickness, bulk elastic field at interface plane are changed more remarkable by correction stress.

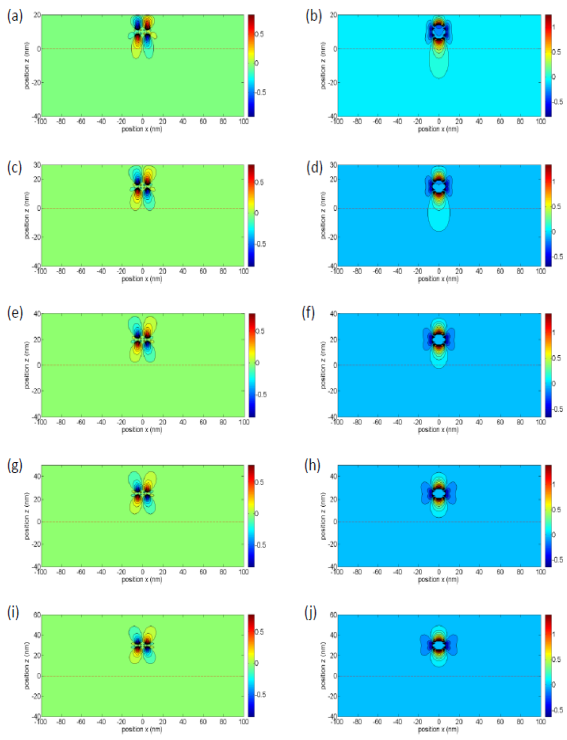

Figure 7: Film thickness effect on elastic fields due to a dislocation loop in the upper Cu film of perfect bonding Cu–Nb film-substrate system. Traction stress field σ_{xz}^{final} and σ_{zz}^{final}: (a)–(b), t=20 nm; (c)–(d), t=30 nm; (e)–(f), t=40 nm; (g)–(h) t=50 nm; (i)–(j), t=60 nm (in unit: GPa).

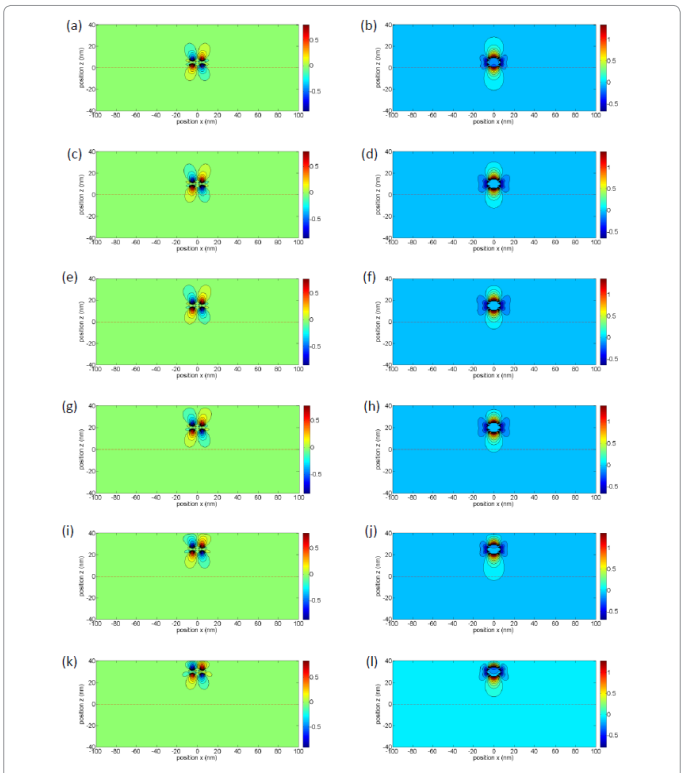

Figure 8: Dislocation loop depth effect on elastic fields due to a dislocation loop in the upper Cu film of perfect bonding Cu–Nb film-substrate system. Traction stress field σ_{xz}^{final} and σ_{zz}^{final}: (a)–(b) d=5 nm; (c)–(d) d=10 nm; (e)–(f) d=15 nm; (g)–(h) d=20 nm; (i)–(j) d=25 nm; (k)–(l) d=30 nm; (in unit: GPa).

Loop Depth Effect on Elastic Field of a Dislocation Loop in the Film Medium

In this subsection, effects of dislocation loop depth within the upper Cu thin film of the Cu-Nb film-substrate system on the elastic field are studied. Besides loop depth, physical parameters of the dislocation loop and perfect bonding film-substrate system are identical to the simulated Cu-Nb film-substrate system example in subsection 3.2. The distance from dislocation loop center to the interface plane is assumed to be: d = 5, 10, 15, 20, 25 and 30 nm, and the film thickness is assumed to be t = 40 nm. The simulation results are shown in Figure 8, and side view of the traction stress σ_{xz} and σ_{zz} are plotted in the oxz plane (y = 0) for the perfect bonding Cu-Nb film-substrate system. It can be concluded from Figure 8 that the interface and free surface can influence the bulk elastic field drastically. With the increase of the distance from dislocation loop center to the interface plane, bulk elastic field at interface plane are changed more remarkable by correction stress.

Conclusion

A semi-analytical calculation approach based on 2D discrete FFT is developed for studying the elastic field due to dislocation loop in perfect bonding thin film-substrate system. Final elastic field is calculated as the linear superposition of bulk stress and the correction stress.

Reliability of the semi-analytical solution is verified by studying the elastic field of dislocation loop within perfect bonding Cu-Nb film-substrate system. Effects of film thickness and loop depth within thin film on the elastic field are analyzed, demonstrating that these two factors have a significant impact on the elastic fields of dislocation loops in the thin film.

Acknowledgement

The research project was Supported by the China Postdoctoral Science Foundation under Grant No. 2015M80091.

References

1. Head AK (1953) The interaction of dislocations. Philosophical Magazine 44: 92-94.
2. Head AK (1953) Edge dislocations in inhomogeneous media. Proc Physical Society 66: 793-801.
3. Head AK (1960) The interaction of dislocations with boundaries and surface films. Australian J of Physics 13: 278-283.
4. Weeks R, Dundurs J, Stippes M (1968) Exact analysis of an edge dislocation near a surface layer. Int J Impact Eng 6: 365-372.
5. Lee MS, Dundurs J (1973) Edge dislocation in a surface layer. Int J Eng Sci 11: 87-94.
6. Öveçoğlu ML, Doerner MF, Nix WD (1987) Elastic interactions of screw dislocations in thin films on substrates. Acta Metallurgica 35: 2947-2957.
7. Kelly PA, O'Connor JJ, Hills DA (1995) The stress field due to dislocation in layered media. J Physics D: Applied Physics 28: 530-534.
8. Savage JC (1998) Displacement field for an edge dislocation in a layered half-space. J Geophysical Research: Solid Earth 103: 2439-2446.
9. Wu X, Weatherly GC (2003) Equilibrium position of misfit dislocations in thin epitaxial films. Semiconductor Sci and Tech 18: 307-311.
10. Wu MS, Wang HY (2007) Solutions for edge dislocation in anisotropic film substrate system by the image method. Mathematics and Mechanics of Solids 12: 183-212.
11. Zhou K, Wu MS (2010) Elastic fields due to an edge dislocation in an isotropic film-substrate by the image method. Acta Mechanica 211: 271-292.
12. Wang HY, Yu Y, Yan SP (2014) Elastic stress fields caused by a dislocation in Ge_xSi_{1-x}/Si film-substrate system. Science China Physics, Mechanics & Astronomy 57: 1078-1089.
13. Salamon NJ, Dundurs J (1971) Elastic fields of a dislocation loop in a two-phase material. J Elasticity 1: 153-163.
14. Salamon NJ, Dundurs J (1977) A circular glide dislocation loop in a two-phase material. J Physics C: Solid State Physics 10: 497-507.
15. Weinberger CR, Aubry S, Lee SW, Nix WD, Cai W (2009) Modelling dislocations in a free-standing thin film. Modelling and Simulation in Mater Sci and Eng 17: 075007.
16. Wu W, Schäublin R, Chen J (2012) General dislocation image stress of anisotropic cubic thin film. J Applied Physics 112: 093522.
17. Volterra, V (1907) Sur l'équilibre des corps élastiques multiplement connexes. Gauthier-Villars Paris 24: 401-517.
18. Devincre B (1995) Three dimensional stress field expressions for straight dislocation segments. Solid State Communications 93: 875-878.
19. Mura T (1987) Micromechanics of Defects in Solids. (2ndedn). Martinus Nijhoff Dordrecht.
20. Bower AF (2012) Applied Mechanics of Solids. CRC Press London.
21. Voigt W (1889) Ueber die Beziehung zwischen den beiden Elasticitätsconstanten isotroper Körper. Annals of Physics 274: 573-587.